

Learning the dynamics of open quantum systems from local measurements

Eyal Bairey,¹ Chu Guo,² Dario Poletti,³ Netanel H. Lindner,¹ and Itai Arad¹

¹*Physics Department, Technion, 3200003, Haifa, Israel*

²*Quantum Intelligence Lab (QI-Lab), Supremacy Future Technologies (SFT), Guangzhou 511340, China*

³*Science and Mathematics Cluster and EPD Pillar, Singapore University of Technology and Design, 8 Somapah Road, 487372 Singapore*

The increasing complexity of engineered quantum systems and devices raises the need for efficient methods to verify that these systems are indeed performing the desired quantum dynamics. Due to the inevitable coupling to external environments, these methods should obtain not only the unitary part of the dynamics, but also the dissipation and decoherence affecting the system's dynamics. Here, we propose a method for reconstructing the Lindbladian governing the Markovian dynamics of open many-body quantum systems, using data obtained from local measurements on their steady states. We show that the number of measurements and computational resources required by the method are polynomial in the system size. For systems with finite-range interactions, the method recovers the Lindbladian acting on each finite spatial domain using only observables within that domain. We numerically study the accuracy of the reconstruction as a function of the number of measurements, type of open-system dynamics and system size. Interestingly, we show that couplings to external environments can in fact facilitate the reconstruction of Hamiltonians composed of commuting terms.

Introduction. Development of quantum simulators and computation devices has been rapidly progressing over the last few years [1]. These developments span a multitude of physical platforms, including ultracold atoms [2–5], trapped ions [6–8], photonic circuits [9–12], Josephson junction arrays [13–17] and more, reaching ever larger complexity. The growth in the complexity of these systems calls for efficient methods to characterize and verify their dynamics. The resources required by these methods, whether classical computations or quantum measurements, should scale polynomially with the number of degrees of freedom in the system.

An isolated quantum system can be characterized by learning its underlying Hamiltonian. This can be achieved by monitoring the dynamics the Hamiltonian generates [18–31], or by measuring local observables in one of its eigenstates or thermal states [32–38]. However, realistic quantum systems are never fully isolated. This raises the need for methods for characterizing the dynamics of *open quantum systems* which are coupled to external environments.

While this important problem received considerable theoretical [39–41] and experimental [40, 42–46] attention, most of the methods proposed so far do not scale polynomially with the number of degrees of freedom. Ref. [18] proposed a scalable method that utilizes short-time measurements of dynamical observables. Here, we propose a scalable method which utilizes local measurements of observables in the *steady states* of open quantum systems.

We focus on open quantum systems evolving under Markovian and local dynamics, for which the evolution can be described by using the Lindblad (or master equation) formalism. While the steady states of such systems generically differ from eigenstates or thermal states of local Hamiltonians, locality imprints strong constraints

on these non-equilibrium steady states. This allows us to build upon and extend the methods of Ref. [38], and propose an efficient method for reconstruction of local Lindbladians from their steady states. In this work, we (i) analyze the conditions for the feasibility and accuracy of such a reconstruction, (ii) show that coupling to a bath can in fact facilitate the reconstruction of certain classes of Hamiltonians, which pose a challenge for methods based on their eigenstates or Gibbs states, and (iii) analyze and numerically study how the accuracy of our method scales with the system's size.

Setting. We consider an open quantum system evolving under local Lindblad dynamics [47, 48],

$$\begin{aligned} \dot{\rho} &= \mathcal{L}(\rho) = \\ &= -i \sum_j [H_j, \rho] + \frac{1}{2} \sum_j \left([L_j \rho, L_j^\dagger] + [L_j, \rho L_j^\dagger] \right), \end{aligned} \quad (1)$$

where each H_j , L_j is a local operator. Throughout this paper, a local operator will be defined as acting on at most k spatially *contiguous* degrees of freedom (e.g. spins). While the Hamiltonian terms H_j are Hermitian, the L_j operators, known as the ‘jump operators’, are generically not. A steady state ρ_s of \mathcal{L} is defined by $\dot{\rho}_s = \mathcal{L}(\rho_s) = 0$. Note that while a Hamiltonian commutes with the density matrix corresponding to any of its eigenstates, the steady state of a Lindbladian is generically unique [49]. Suppose that we prepare many copies of ρ_s and measure expectation values of local observables in the state ρ_s . Can \mathcal{L} be recovered using the data obtained from these measurements?

As we show below, the expectation value of any local observable in the state ρ_s imposes a constraint on the parameters that describe the local Lindbladian. Since the number of such parameters scales polynomially in the system size, it is plausible that by considering a sufficiently large number of such local observables (polynomi-

ally many), we should be able to recover the parameters of the underlying Lindbladian.

Algorithm. We begin by choosing a basis of local Hermitian operators for the unitary dynamics $\{h_i\}$, and a basis of local operator *pairs* for the dissipative dynamics $\{(l_r, l_s)\}$. Expanding the dynamics in this operator basis (see Supplemental Materials), Eq. (1) becomes

$$\dot{\rho} = -i \sum_i c_i [h_i, \rho] + \sum_{r,s} \frac{c_{rs}}{2} ([l_r \rho, l_s^\dagger] + [l_r, \rho l_s^\dagger]), \quad (2)$$

with real coefficients c_j , and c_{rs} forming a complex-valued positive semidefinite matrix. The locality of the Lindbladian restricts the pairs of non-zero elements of c_{rs} ; e.g., if the jump operators L_j are on-site, c_{rs} vanishes whenever l_r, l_s act on different sites. Our goal is to infer the values of the non-zero coefficients c_j, c_{rs} .

To this end, we identify a set of local constraints that apply to any steady state ρ_s of \mathcal{L} . Since ρ_s is a steady state, the expectation value $\langle A \rangle \stackrel{\text{def}}{=} \text{Tr}(A\rho_s)$ of any observable must be time-independent,

$$\text{Tr}(A\dot{\rho}_s) = 0. \quad (3)$$

Plugging in Eq. (2) and using the cyclic properties of the trace, $\text{Tr}(ABC) = \text{Tr}(CAB)$ and $\text{Tr}(A[B, C]) = \text{Tr}(C[A, B])$, we obtain the linear constraint

$$-\sum_i c_i \langle i[A, h_i] \rangle + \sum_{r,s} \frac{c_{r,s}}{2} \sum_{r,s} \langle [l_r, A] l_s^\dagger + l_r [A, l_s^\dagger] \rangle = 0, \quad (4)$$

where the expectation values are taken with respect to the steady state ρ_s . For any operator A , Eq. (4) yields a homogeneous linear equation for the parameters $c_j, c_{r,s}$. Using a set of constraint operators $\{A_n\}$, we obtain a homogeneous system of linear equations which the true Lindbladian coefficients must satisfy. When the number of equations reaches the number of unknowns, we expect these equations to have a unique solution, revealing the Lindbladian parameters up to an overall multiplicative scalar.

Importantly, assuming that local A_n operators are chosen, the constraints derived from Eq. (4) are local in two ways. First, these constraints involve only local observables, which are easier to measure in most experimental settings. Second, if the A_n operators act only within a given region, they commute with all the Lindblad terms that are supported outside that region. This allows to recover the Lindbladian of a region from measurements of that region alone.

In practice, we concatenate the Hamiltonian parameters c_j and the dissipative parameters $c_{r,s}$ into a single vector \vec{c} . In this notation, Eq. (4) takes the form

$$\vec{k}^T \vec{c} = 0 \quad (5)$$

for a corresponding vector of expectation values \vec{k} . Since $c_{r,s}$ is Hermitian, its upper and lower parts are redundant; each pair of off-diagonal elements contributes only

a single pair of real parameters, $\text{Re}\{c_{r,s}\} = \frac{1}{2}(c_{r,s} + c_{s,r})$ and $\text{Im}\{c_{r,s}\} = \frac{1}{2i}(c_{r,s} - c_{s,r})$. Thus, \vec{c} is a real vector with four types of elements: Hamiltonian coefficients c_j , diagonal dissipative coefficients $c_{r,r}$, and the real and imaginary parts of the off-diagonal dissipative coefficients $c_{r,s}$ for $r > s$.

Repeating this procedure for a set of constraints $\{A_n\}_{n=1}^N$, we obtain a system of linear equations,

$$K\vec{c} = 0, \quad (6)$$

where K is an $N \times M$ matrix of expectation values (see Supplemental Materials), with N the number of constraints and M the number of unknown parameters. Its rows correspond to the constraint operators A_n , and its columns to different generators of the dynamics.

Error analysis. Assuming that the elements of K are known exactly, our method succeeds if the equation $K\vec{c} = 0$ has a *unique* solution. Put differently, the spectrum of singular values of K must contain a single zero. More generally, in the presence of noise, the spectrum of K determines the difficulty, or noise sensitivity, of the Lindbladian reconstruction. Suppose that each observable is only known to an additive error $\epsilon > 0$ [50]. The corresponding noise in the coefficients of K will lead to an error in the recovered Lindbladian. We measure the distance Δ between two Lindbladians by the L_2 distance between their coefficient vectors \vec{c} ; since the Lindbladian is only recovered up to a multiplicative scalar, we use the normalized coefficient vectors $\hat{c} = \vec{c}/\|\vec{c}\|$, so that

$$\Delta = \|\hat{c}_{\text{recovered}} - \hat{c}_{\text{true}}\|_2. \quad (7)$$

Using perturbation theory, we estimated in Ref. [38] the reconstruction error due to independent random noise with standard deviation ϵ added to each element of K ,

$$\Delta^{\text{est}} = \epsilon \sqrt{\sum_{m>0} \lambda_m^{-1}}, \quad (8)$$

where λ_m are the eigenvalues of $K^T K$ [51] (i.e., the squared singular values of K). Based on this perturbative result, we choose the ratio Δ/ϵ as our figure of merit for the difficulty of the reconstruction: the smaller it is, the fewer measurements of each observable are required to recover the Lindbladian to a given accuracy. We verified numerically that for a fixed K , this ratio remains approximately constant over several orders of magnitudes of ϵ , as long as $\Delta < 10^{-2}$ (see inset of Fig. 1a).

Recovery of random local Lindbladians. We apply our method for the reconstruction of random local Lindbladians from their respective steady states. We start by focusing on chains of $\Lambda = 6$ spins with random local interactions and dissipation. We consider Lindbladians of the form given in Eq.(1) with local Hamiltonian terms

$$H_j = \sum_{\alpha=1}^3 c_{j,\alpha} \sigma_j^\alpha + \sum_{\alpha,\beta=1}^3 c_{j,\alpha,\beta} \sigma_j^\alpha \sigma_{j+1}^\beta, \quad (9)$$

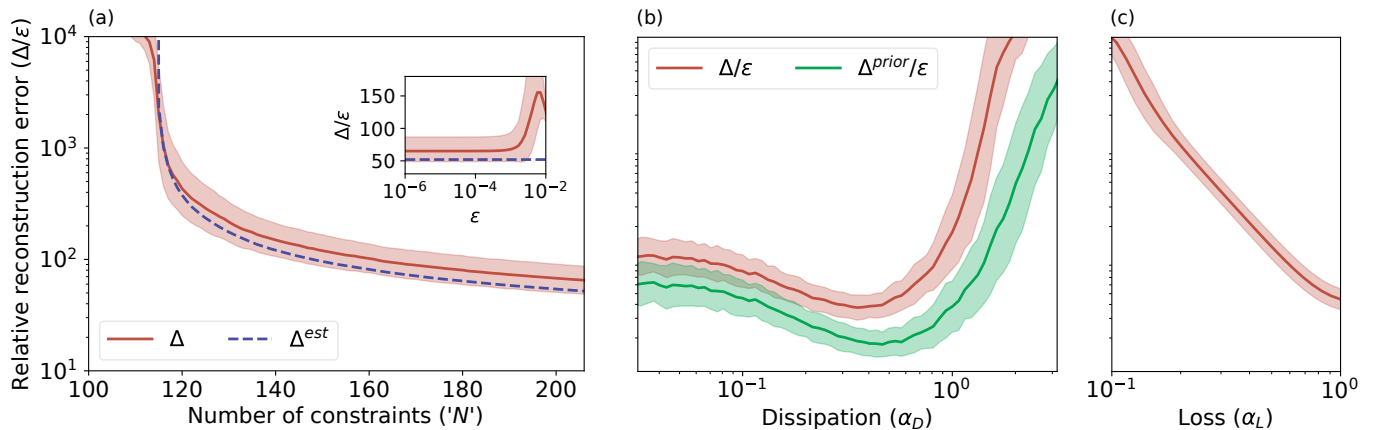


FIG. 1. Reconstruction of local Lindbladians from their steady states. We generated steady states of random Lindbladians on chains of $\Lambda = 6$ spins and measured local observables given by Eq. (4) for a set of constraint operators $\{A_n\}_{n=1}^N$. We then recovered the Lindbladians from these observables by solving Eq. (6), adding a small random noise of order $\epsilon = 10^{-4}$ to each observable, and measured the error Δ in the recovered Lindbladians [see Eq. (7)]. (a) Relative reconstruction error (Δ/ϵ) of random Lindbladians [Eqs. (9, 10)] as a function of the number of constraints (red; shaded area indicates error bars). Recovery succeeded once the number of constraints N approached the number of unknowns M ; its accuracy improved as more constraints were added, following the estimate of Eq. (8). Here, the ratio between the standard deviations of the Hamiltonian and dissipative terms was fixed to $\alpha_D = \frac{1}{\sqrt{2}}$. Inset: the relative reconstruction error Δ/ϵ with all 3-local constraints as a function of the noise magnitude ϵ . The error followed the prediction of Eq. (8) as long as $\Delta \ll 1$. (b) Relative reconstruction error as a function of the dissipation strength α_D . Here we used all constraints A_n acting on up to 3 consecutive sites. Addition of weak dissipation improved the Lindbladian recovery, which was optimal at $\alpha_D \approx 0.5$. A lower reconstruction error was achieved when the Hamiltonian was known (green; Δ^{prior}/ϵ). (c) Dependence of the reconstruction error on the type of dissipation. We used the same ensemble of random Hamiltonians, with dissipation given by Eq. (12), and α_L interpolating between loss and dephasing. When dissipation is almost entirely due to dephasing, $\alpha_L \rightarrow 0$, the steady state is close to being fully mixed; consequently, recovery improves with increasing loss (increasing α_L). All results were averaged over 300 random Lindbladians, with error bars indicating one standard deviation; means and standard deviations were calculated after taking the log.

and on-site jump operators L_j given by

$$L_j = \sum_{\alpha=1}^3 d_{j,\alpha} \sigma_j^\alpha. \quad (10)$$

We choose open boundary conditions $c_{L,\alpha,\beta} = 0$, and draw the remaining Hamiltonian coefficients from a Gaussian distribution with zero mean and unit variance, setting the energy scale for what follows. The real and imaginary parts of the dissipative coefficients $d_{j,\alpha}$ are similarly drawn from a Gaussian distribution, with mean zero and standard deviation $\alpha_D = \frac{1}{\sqrt{2}}$.

We obtain the steady state of each random Lindbladian \mathcal{L} by exactly diagonalizing it as a superoperator. We then attempt to recover \mathcal{L} using an increasing number N of constraints A_n . We use all the constraints A_n on single sites and nearest neighbors, and add constraints supported on three consecutive sites in random order. To quantify the reconstruction difficulty in practical settings, we add a small independent, Gaussian noise to each observable with mean zero and standard deviation $\epsilon = 10^{-4}$, and measure the resulting recovery error Δ . As soon as the number of constraints approaches the number of unknowns, the relative reconstruction error Δ/ϵ drops and we recover the Lindbladian (Fig. 1a). The error decreases with the number of constraints, following

the estimate of Eq. (8).

Efficiency of recovery and properties of the Lindbladian. Next, we study how the accuracy of the method depends on the type and strength of the dissipative terms appearing in the Lindbladian. First, we vary the magnitude α_D of the dissipative terms appearing in Eq. (10) relative to the Hamiltonian terms. We repeat the recovery experiment on the steady states of these different dynamics, using all 3-local constraints A_n . We find that the accuracy of the method improves upon adding weak dissipation to a Hamiltonian; the recovery is optimal when the dissipative terms are comparable in magnitude to the Hamiltonian terms (Fig. 1b, red). Due to our choice of single-site jump operators, Eq. (10), steady states at the strong dissipation limit approach product states. Since any product state is a steady state of many different Lindbladians, the reconstruction error diverges for $\alpha_D \rightarrow \infty$; this divergence of the error is cured when two-site nearest-neighbor jump operators are added (see Supplemental Materials).

In practical situations, the jump operators L_j may be unknown even if the Hamiltonian is well-characterized. We can incorporate prior knowledge about the Hamiltonian by turning Eq. (4) into the non-homogeneous con-

straint

$$\sum_{r,s} \frac{c_{r,s}}{2} \sum_{r,s} \langle [l_r, A] l_s^\dagger + l_r [A, l_s^\dagger] \rangle = \langle i [A, H] \rangle, \quad (11)$$

where the RHS is directly obtained by measurements. The dissipative coefficients $c_{r,s}$ are then obtained by solving a system of non-homogeneous linear equations (see Supplemental Materials). Fig. 1b shows that recovery with such prior knowledge of the Hamiltonian achieves a lower reconstruction error of the Lindbladian (green curve).

Next, we study the interplay of different dissipation types. We consider a Lindbladian \mathcal{L} which consists of single-site jump operators of two kinds,

$$L_{j,L} = \alpha_L \sigma_j^-, \quad L_{j,D} = (1 - \alpha_L) \sigma_j^z, \quad (12)$$

where $\sigma^- \stackrel{\text{def}}{=} \frac{1}{2}(\sigma^x - i\sigma^y)$. The “loss” $L_{j,L}$ relaxes the system towards a pure steady state, e.g. due to loss of particles; the “dephasing” $L_{j,D}$ scrambles relative phases between pure states in a specific basis. We tune the parameter $0 \leq \alpha_L \leq 1$ to interpolate the relative weights of the loss and dephasing. In addition, \mathcal{L} contains Hamiltonian terms of the form (9), with coefficients drawn from a Gaussian distribution with zero mean and unit variance. We then attempt to recover both the Hamiltonian and the jump operators from the steady state of \mathcal{L} using all 3-local constraints A_n , without assuming that the form of the on-site jump operators is known.

We find that reconstruction of strongly dephasing Lindbladians is hard (Fig. 1c). This is expected: for $\alpha_L \ll 1$, the steady state is close to a fully mixed state $\rho \propto \mathbb{1}$, compatible with any Lindbladian with Hermitian jump operators. As the loss intensifies, $\|\mathcal{L}(\mathbb{1})\| \propto \alpha_L^2$; correspondingly, Fig. 1c shows that the reconstruction error decreases as α_L^{-2} (see also Supplemental Materials), indicating that the steady state becomes more informative.

Loss facilitates learning of hard Hamiltonians. Motivated by the insight that loss can lead to non-trivial steady states, we investigate whether dissipation can aid in learning Hamiltonians that could not be recovered from their steady states. In particular, we consider classical Hamiltonians with random nearest-neighbor interactions in the X-basis alone,

$$H_{cl}^x = \sum_{j=1}^{\Lambda} b_j \sigma_j^x + \sum_{j=1}^{\Lambda-1} J_j \sigma_j^x \sigma_{j+1}^x, \quad (13)$$

whose coefficients are drawn from a Gaussian distribution with zero mean and unit variance. Any state ρ diagonal in the X-basis is a steady state of H_{cl}^x , revealing no information about its coefficients. We therefore add on-site jump operators

$$L_j = 2\sigma_j^-, \quad (14)$$

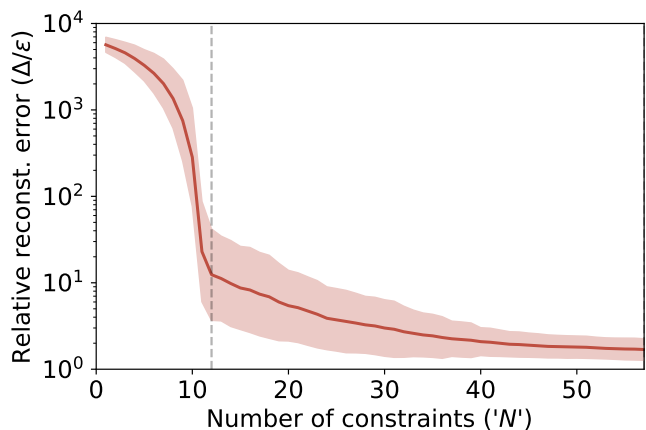


FIG. 2. Loss facilitates learning of hard Hamiltonians: error in the reconstruction of classical Hamiltonians from steady states of dissipative dynamics, as a function of the number of constraints N . We generate random classical Ising Hamiltonians on a one-dimensional chain with $\Lambda = 6$ spins [Eq. (13)]. While these Hamiltonians are impossible to learn from a generic steady state, the addition of loss $L_j = \sigma_j^-$ allows to extract their coupling parameters. Due to the small number of unknowns, recovery is easy, and single-site constraint operators suffice (dashed vertical line; corresponds to 2-local measured observables).

so that the dynamics of \mathcal{L} are comprised of Hamiltonian dynamics in the X basis and loss in the Z basis. We then attempt to recover H from the steady state of \mathcal{L} , assuming that the jump operators L_j are known.

We find that the addition of controlled loss facilitates efficient learning of the classical Hamiltonians of Eq. (13). Due to the small number of unknowns, single-site constraint operators σ_j^y, σ_j^z are sufficient to recover H (σ_j^x are not required as they commute with H). Moreover, a modest number of measurements of each observable suffices: when nearest-neighbor constraints are added, the accuracy of the recovered Hamiltonian approaches the measurement accuracy (Fig. 2).

System-size scaling. Finally, we demonstrate that our method can recover Lindbladians on long spin chains. Using MPO simulations [52, 53], we obtain steady states of the random Lindbladians considered in Eqs. (9), (10) on chains with $\Lambda = 100$ spins (see Supplemental Materials for details). To study the system-size scaling of our method, we focus on subsystems of increasing sizes: we begin with the 6 leftmost spins and add 4 spins in each step, eventually covering the whole chain. We then attempt to recover the Lindbladian of each of these subsystems from observables within that subsystem only, using all 3-local constraints.

To recover the full Lindbladians of these increasingly large subsystems, we employ two different approaches. In the first approach, we partition the subsystem to overlapping patches of 6 spins, and recover the Lindbladian on each patch independently. The recovery does not de-

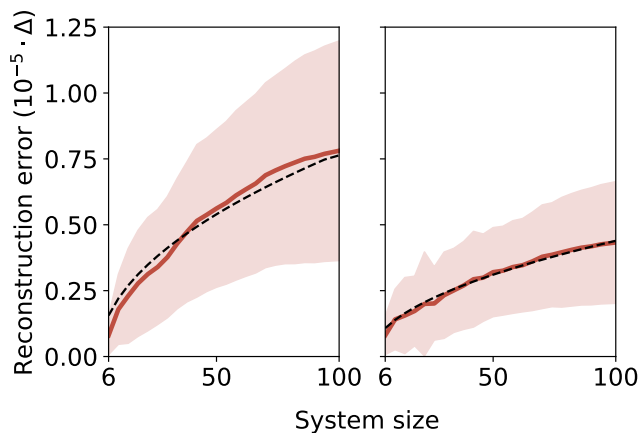


FIG. 3. Reconstruction of Lindbladians on large spin chains: system-size scaling of the reconstruction error. We obtained the steady states of the random Lindbladians described in Eqs. (9), (10) on $\Lambda = 100$ spins. (left) We recovered the Lindbladians on spatial patches of 6 spins, with overlaps of 2 sites between consecutive patches. We used all constraints supported on up to 3 consecutive sites in the interior of each patch (middle 4 sites for bulk patches). We then stitched consecutive n patches to obtain the full Lindbladian on subsystems of increasing length. The reconstruction error increased as the square root of the number of patches (dashed line). (right) As a different approach, we built a single large constraint matrix for each subsystem, and obtained the error as a function of subsystem size; this approach yielded a slightly smaller reconstruction error, still scaling as the square root of subsystem size (dashed line).

termine the overall scale factor of the Lindbladian on the patch; we therefore re-scale the coefficients of neighboring patches according to the coefficients of their shared terms (see Supplemental Materials). In the second approach, we apply our method directly on the whole subsystem, forming a large constraint matrix K which grows with the subsystem size.

Both approaches successfully recover the full-system Lindbladian using the same set of measurements. Here we do not add measurement noise; the error in a single patch ($\approx 10^{-6}$) is controlled by the numerical precision of the MPO steady state. Due to the uncertainty in the coefficients shared between each pair of patches, the norm of the recovered Lindbladian performs a random walk, leading to a total error growing as the square root of the number of patches (Fig. 3, left). We find the same square root system-size scaling of the reconstruction error in the second, direct approach (Fig. 3, right). This suggests that to recover the Lindbladian of a system of length Λ to a fixed accuracy, it is sufficient to measure each observable to an additive error of order $\Lambda^{-1/2}$.

Conclusions. Near-term intermediate-scale quantum devices [1] are invariably subject to noise and coupled to their environments. While tomographic methods can characterize gates acting on a few isolated qubits [54, 55],

cross-talk between qubits necessitates holistic methods that identify the sources of error in an entire device [56].

We propose a scalable method for recovering unknown dynamics of many-body open quantum systems from local measurements of their steady states. Our method allows to extract the generator of dynamics of each subsystem using only measurements within that subsystem. Thus, to recover the dynamics of a large system of length Λ , our method requires only $O(\Lambda)$ observables. Our findings indicate that measuring each of these observables $O(\Lambda)$ times suffices to recover the dynamics of the whole system to a fixed accuracy, amounting to $O(\Lambda^2)$ measurements in total. With the addition of controlled loss, our method allows to characterize Hamiltonians consisting of commuting terms, such as topological quantum error correcting codes (similarly to Ref. [57]). We stress that the method is independent on the dimensionality of the local Hilbert space, and is effective also for bosonic systems with an infinite-dimensional local Hilbert space.

Having demonstrated that open quantum system dynamics can often be learned from their steady states, it is important to obtain rigorous bounds on the number of measurements required for the learning process. Such bounds could be obtained by identifying conditions under which our constraint matrix is guaranteed to be gapped. It could also be interesting to study our method as a means to certify quantum states prepared as the steady states of given quantum dynamics. Finally, adapting our method to the setting of quantum circuits may yield means to certify, characterize and benchmark quantum devices.

We thank Yotam Shapira for useful discussions. E. B. and N. L. acknowledge financial support from the European Research Council (ERC) under the European Union Horizon 2020 Research and Innovation Programme (Grant Agreement No. 639172). D.P. acknowledges support from the Singapore Ministry of Education, Singapore Academic Research Fund Tier-II (project MOE2018-T2-2-142). N. L. acknowledges support from the People Programme (Marie Curie Actions) of the European Union's Seventh Framework Programme (No. FP7/2007–2013) under REA Grant Agreement No. 631696 and the Defense Advanced Research Projects Agency through the DRINQS program, grant No. D18AC00025. The content of the information presented here does not necessarily reflect the position or the policy of the U.S. government, and no official endorsement should be inferred. I.A. acknowledges the support of the Israel Science Foundation (ISF) under the Individual Research Grant No. 1778/17.

BIBLIOGRAPHY

- [1] J. Preskill, *Quantum* **2**, 79 (2018).

- [2] C. Monroe, “Quantum information processing with atoms and photons,” (2002).
- [3] I. Bloch, J. Dalibard, and W. Zwerger, *Reviews of Modern Physics* (2008), 10.1103/RevModPhys.80.885.
- [4] C. Gross and I. Bloch, “Quantum simulations with ultracold atoms in optical lattices,” (2017).
- [5] H. Bernien, S. Schwartz, A. Keesling, H. Levine, A. Omran, H. Pichler, S. Choi, A. S. Zibrov, M. Endres, M. Greiner, V. Vuletic, and M. D. Lukin, *Nature* (2017), 10.1038/nature24622.
- [6] J. I. Cirac and P. Zoller, *Physical Review Letters* (1995), 10.1103/PhysRevLett.74.4091.
- [7] R. Blatt and C. F. Roos, “Quantum simulations with trapped ions,” (2012).
- [8] C. Monroe and J. Kim, “Scaling the ion trap quantum processor,” (2013).
- [9] P. Kok, W. J. Munro, K. Nemoto, T. C. Ralph, J. P. Dowling, and G. J. Milburn, *Reviews of Modern Physics* (2007), 10.1103/RevModPhys.79.135.
- [10] A. Aspuru-Guzik and P. Walther, “Photonic quantum simulators,” (2012).
- [11] F. Flamini, N. Spagnolo, and F. Sciarrino, *Reports on Progress in Physics* **82**, 016001 (2019).
- [12] S. Takeda and A. Furusawa, *APL Photonics* **4**, 060902 (2019).
- [13] J. Q. You and F. Nori, “Superconducting circuits and quantum information,” (2005).
- [14] A. A. Houck, H. E. Türeci, and J. Koch, *Nature Physics* (2012), 10.1038/nphys2251.
- [15] M. H. Devoret and R. J. Schoelkopf, “Superconducting circuits for quantum information: An outlook,” (2013).
- [16] G. Wendin, “Quantum information processing with superconducting circuits: A review,” (2017).
- [17] C. Neill, P. Roushan, K. Kechedzhi, S. Boixo, S. V. Isakov, V. Smelyanskiy, A. Megrant, B. Chiaro, A. Dunsworth, K. Arya, R. Barends, B. Burkett, Y. Chen, Z. Chen, A. Fowler, B. Foxen, M. Giustina, R. Graff, E. Jeffrey, T. Huang, J. Kelly, P. Klimov, E. Lucero, J. Mutus, M. Neeley, C. Quintana, D. Sank, A. Vainsencher, J. Wenner, T. C. White, H. Neven, and J. M. Martinis, *Science* (2018), 10.1126/science.aao4309.
- [18] M. P. Da Silva, O. Landon-Cardinal, and D. Poulin, *Phys. Rev. Lett.* **107** (2011), 10.1103/PhysRevLett.107.210404.
- [19] D. Burgarth, K. Maruyama, and F. Nori, *Phys. Rev. A* **79** (2009), 10.1103/PhysRevA.79.020305.
- [20] C. Di Franco, M. Paternostro, and M. S. Kim, *Phys. Rev. Lett.* **102** (2009), 10.1103/PhysRevLett.102.187203.
- [21] A. Shabani, M. Mohseni, S. Lloyd, R. L. Kosut, and H. Rabitz, *Phys. Rev. A* **84** (2011), 10.1103/PhysRevA.84.012107.
- [22] J. Zhang and M. Sarovar, *Phys. Rev. Lett.* **113**, 080401 (2014).
- [23] S. T. Wang, D. L. Deng, and L. M. Duan, *New Journal of Physics* **17** (2015), 10.1088/1367-2630/17/9/093017.
- [24] L. E. De Clercq, R. Oswald, C. Flühmann, B. Keitch, D. Kienzler, H. Y. Lo, M. Marinelli, D. Nadlinger, V. Negnevitsky, and J. P. Home, *Nat. Comm.* **7** (2016), 10.1038/ncomms11218.
- [25] A. Sone and P. Cappellaro, *Physical Review A* **95** (2017), 10.1103/PhysRevA.95.022335.
- [26] Y. Wang, D. Dong, B. Qi, J. Zhang, I. R. Petersen, and H. Yonezawa, *IEEE Transactions on Automatic Control* **63**, 1388 (2018).
- [27] C. E. Granade, C. Ferrie, N. Wiebe, and D. G. Cory, *New Journal of Physics* **14** (2012), 10.1088/1367-2630/14/10/103013.
- [28] N. Wiebe, C. Granade, C. Ferrie, and D. G. Cory, *Phys. Rev. Lett.* **112** (2014), 10.1103/PhysRevLett.112.190501.
- [29] N. Wiebe, C. Granade, C. Ferrie, and D. G. Cory, *Phys. Rev. A* **89** (2014), 10.1103/PhysRevA.89.042314.
- [30] N. Wiebe, C. Granade, and D. G. Cory, *New Journal of Physics* **17** (2015), 10.1088/1367-2630/17/2/022005.
- [31] J. Wang, S. Paesani, R. Santagati, S. Knauer, A. A. Gentile, N. Wiebe, M. Petruzzella, J. L. O’Brien, J. G. Rarity, A. Laing, and M. G. Thompson, *Nat. Phys.* **13**, 551 (2017).
- [32] K. Rudinger and R. Joynt, *Phys. Rev. A* **92** (2015), 10.1103/PhysRevA.92.052322.
- [33] M. Kieferová and N. Wiebe, *Physical Review A* (2017), 10.1103/PhysRevA.96.062327.
- [34] X.-L. Qi and D. Ranard, arXiv:1712.01850 (2017).
- [35] E. Chertkov and B. K. Clark, *Physical Review X* **8**, 031029 (2018).
- [36] M. Greiter, V. Schnells, and R. Thomale, *Physical Review B* **98**, 081113 (2018).
- [37] H. J. Kappen, arXiv:1803.11278 (2018).
- [38] E. Bairey, I. Arad, and N. H. Lindner, *Physical Review Letters* **122** (2019), 10.1103/PhysRevLett.122.020504.
- [39] I. L. Chuang and M. A. Nielsen, *Journal of Modern Optics* **44-11**, 2455 (1997).
- [40] N. Boulant, T. F. Havel, M. A. Pravia, and D. G. Cory, *Physical Review A - Atomic, Molecular, and Optical Physics* **67**, 12 (2003).
- [41] J. Zhang and M. Sarovar, *Physical Review A - Atomic, Molecular, and Optical Physics* **91** (2015), 10.1103/PhysRevA.91.052121.
- [42] A. M. Childs, I. L. Chuang, and D. W. Leung, *Physical Review A. Atomic, Molecular, and Optical Physics* **64**, 123141 (2001).
- [43] M. Howard, J. Twamley, C. Wittmann, T. Gaebe, F. Jelezko, and J. Wrachtrup, *New Journal of Physics* **8** (2006), 10.1088/1367-2630/8/3/033.
- [44] N. Akerman, S. Kotler, Y. Glickman, and R. Ozeri, *Physical Review Letters* **109** (2012), 10.1103/PhysRevLett.109.103601.
- [45] Y. Glickman, S. Kotler, N. Akerman, and R. Ozeri, “Emergence of a measurement basis in atom-photon scattering,” (2013).
- [46] Q. Ficheux, S. Jezouin, Z. Leghtas, and B. Huard, *Nature Communications* **9** (2018), 10.1038/s41467-018-04372-9.
- [47] V. Gorini, *Journal of Mathematical Physics* **17**, 821 (1976).
- [48] G. Lindblad, *Communications in Mathematical Physics* **48**, 119 (1976).
- [49] D. E. Evans, *Communications in Mathematical Physics* **54**, 293 (1977).
- [50] For example, if each observable is measured experimentally using n_s copies of ρ , its expectation value is known up to random noise of order $\epsilon \sim 1/\sqrt{n_s}$.
- [51] In particular, the recovery error is dominated by the gap λ_1 of the constraint matrix, since $\Delta_{est} \leq \sqrt{M\lambda_1^{-1}}$.
- [52] J. Cui, J. I. Cirac, and M. C. Bañuls, *Physical Review Letters* **114** (2015), 10.1103/PhysRevLett.114.220601.
- [53] A. H. Werner, D. Jaschke, P. Silvi, M. Kliesch, T. Calarco, J. Eisert, and S. Montangero,

Physical Review Letters **116** (2016), 10.1103/PhysRevLett.116.237201.

- [54] S. T. Merkel, J. M. Gambetta, J. A. Smolin, S. Poletto, A. D. Córcoles, B. R. Johnson, C. A. Ryan, and M. Steffen, *Physical Review A - Atomic, Molecular, and Optical Physics* (2013), 10.1103/PhysRevA.87.062119.
- [55] R. Blume-Kohout, J. K. Gamble, E. Nielsen, K. Rudinger, J. Mizrahi, K. Fortier, and P. Maunz, *Nature Communications* (2017), 10.1038/ncomms14485.
- [56] T. J. Proctor, A. Carignan-Dugas, K. Rudinger, E. Nielsen, R. Blume-Kohout, and K. Young, [arXiv:1807.07975](https://arxiv.org/abs/1807.07975) (2018).
- [57] A. Valenti, E. van Nieuwenburg, S. Huber, and E. Greplova, [arXiv:1907.02540](https://arxiv.org/abs/1907.02540) (2019).

SUPPLEMENTARY MATERIALS

Expanding the Lindblad dynamics in a fixed set of operators: derivation of Eq. (2)

Formally, to derive Eq. (2) from Eq. (1), we first expand each local Hamiltonian term in a fixed basis of local operators

$$H_j = \sum_i c_i^{(j)} h_i, \quad (\text{S1})$$

so that the unitary evolution term becomes

$$\sum_j [H_j, \rho] = \sum_i c_i [h_i, \rho] \quad (\text{S2})$$

with

$$c_i = \sum_j c_i^{(j)}. \quad (\text{S3})$$

Similarly, we expand each jump operator in a fixed basis of local operators

$$L_j = \sum_i c_r^{(j)} l_r, \quad (\text{S4})$$

so that the dissipative dynamics may be rewritten as

$$\begin{aligned} \frac{1}{2} \sum_j \left([L_j \rho, L_j^\dagger] + [L_j, \rho L_j^\dagger] \right) &= \\ &= \sum_{r,s} \frac{c_{rs}}{2} \left([l_r \rho, l_s^\dagger] + [l_r, \rho l_s^\dagger] \right), \end{aligned}$$

where

$$c_{rs} = \sum_j c_r^{(j)} (c_s^{(j)})^* \quad (\text{S5})$$

forms a positive semi-definite matrix by definition.

Exact form of the constraint matrix

As derived in Eqs (4-6), the elements of the constraint matrix K are expectation values of different observables. The explicit form of the element $K_{n,m}$ varies, depending on the term in the expansion of the Lindbladian in Eq. (2) which corresponds to the index m : (i) coefficients c_j of Hamiltonian terms; (ii) diagonal entries of the matrix of dissipative coefficients c_{rr} ; (iii) the real part of the off-diagonal dissipative coefficients $\frac{1}{2} \text{Re}\{c_{rs} + c_{sr}\}$; (iiii) the imaginary part of the off-diagonal dissipative coefficients $\frac{1}{2i} \text{Re}\{c_{rs} - c_{sr}\}$. Explicitly, the matrix elements $K_{n,m}$ are given by (see also Fig. S1):

$$K_{n,m} = \begin{cases} -\langle i [A_n, h_j] \rangle & c_j \\ \frac{1}{2} \langle [l_r, A_n] l_s^\dagger + l_r [A_n, l_s^\dagger] \rangle & c_{rr} \\ \frac{1}{2} (\langle [l_r, A_n] l_s^\dagger + l_r [A_n, l_s^\dagger] \rangle + \{r \leftrightarrow s\}) & \text{Re}\{c_{rs}\}; r > s \\ \frac{i}{2} (\langle [l_r, A_n] l_s^\dagger + l_r [A_n, l_s^\dagger] \rangle - \{r \leftrightarrow s\}) & \text{Im}\{c_{r,s}\}; r > s. \end{cases} \quad (\text{S6})$$

Error analysis

Recovery of strongly dissipating Lindbladians

In Fig. 1b, it appears that the recovery error diverges when the relative magnitude of the dissipative terms is large $\alpha_D > 1$. We conjectured that this divergence does not indicate that recovery is generically impossible in the limit of strong dissipation; rather, it is an artifact of the choice of strictly single-site dissipation we simulated.

To verify this conjecture, we added nearest-neighbor jump operators to our random Lindbladians

$$L_j = \sum_{\alpha=1}^3 d_{j,\alpha} \sigma_j^\alpha + d_{j,x,x} \sigma_j^x \sigma_{j+1}^x + d_{j,y,y} \sigma_j^y \sigma_{j+1}^y, \quad (\text{S7})$$

with all coefficients drawn from a Gaussian distribution with mean zero and standard deviation α_D ; for the Hamiltonian terms, we used the same random nearest-neighbor interactions of Eq. (9). We then recovered these Lindbladians from their steady states, assuming that the form of the jump operators is known but their coefficients are not. We found that the reconstruction error of these Lindbladians saturates at large α_D (Fig. S2, blue); thus, the divergence of the reconstruction error is cured when entangling jump operators are added.

Recovery error: results vs. expectation

The relative recovery error Δ/ϵ we find in Fig. 1a is slightly higher (by a factor of ≈ 1.25) than the estimate

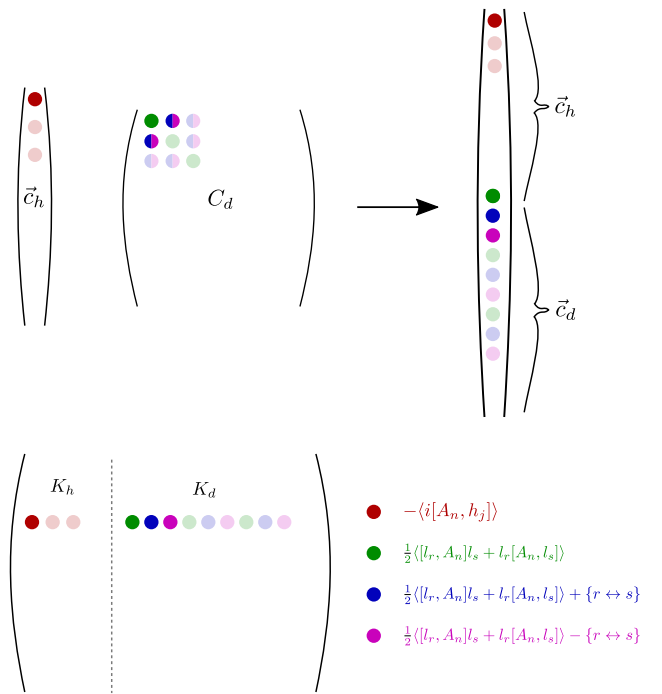


FIG. S1. Top: we concatenate the Hamiltonian coefficients \vec{c}_h and the matrix of dissipative coefficients C_d into a long vector of coefficients for the Lindblad evolution. Off-diagonal entries of C_d are split into their real and imaginary parts (blue and magenta, correspondingly). Bottom: the constraint matrix is composed of a vertical block corresponding to Hamiltonian terms K_h , and a vertical block corresponding to dissipative terms K_d . Entries corresponding to Hamiltonian terms are given by their commutators with the constraint operators (red); the formula for the dissipative entries varies between the diagonal entries of the dissipative matrix C_d (green), and the real (blue) and imaginary (magenta) entries of C_d .

of Eq. (8), derived in Ref. [38]. In contrast to our results in this work, in Ref. [38] the obtained recovery error was lower than the prediction of the same estimate, which is indeed expected to be pessimistic due to the use of Jensen's inequality.

We believe the difference is due to the different noise model used in both papers: here we add noise to each measured observable, while in [38] we added independent noise to each one of the entries of K (even when they contain the same observable). In Ref. [38], we wished to test the theoretical validity of the error estimate. The estimate assumes that the noise in each entry of the constraint matrix K is independent, and we thus added an independent random noise to each of its entries. Realistically though, noise is incurred in each measured observable. Since many different entries of K feature the same observable, this introduces correlations between the noise in different entries.

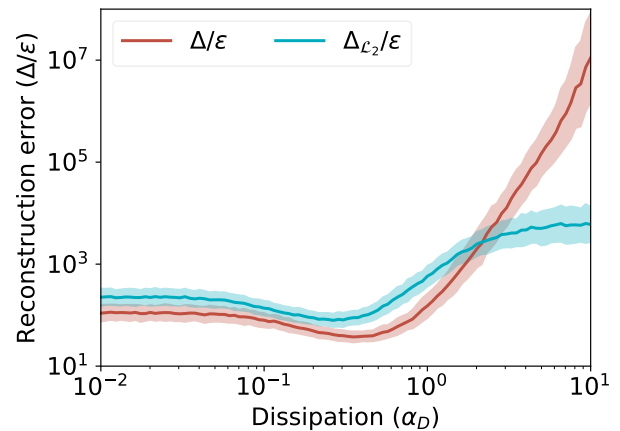


FIG. S2. Entangling jump operators facilitate learning of strongly dissipative dynamics. Reconstruction error as a function of dissipation strength α_D of Lindbladians with nearest-neighbor Hamiltonian terms [Eq. (9)]; for the dissipation, we took either strictly single-site jump operators (red), as in main text [Eq. (10)]; or both single-site and nearest-neighbor jump operators (blue) [Eq. (S7)]. The divergence of the error at the strong dissipation limit is cured when nearest-neighbor jump operators are added. Here, we added a smaller noise than in the main text ($\epsilon = 10^{-8}$ rather than 10^{-4}) to probe the behavior at large values of Δ/ϵ .

Scaling of the reconstruction error with loss-to-dephasing ratio

We argued that Fig. 1c confirms the theoretical expectation that the reconstruction error scale as α_L^{-2} for small values of the loss-to-dephasing ratio α_L . However, the curve in Fig. 1c did not show a clear power law for small α_L , since the reconstruction error approached large values of order 1. We thus repeated these simulations with weaker measurement noise ($\epsilon = 10^{-8}$ compared to $\epsilon = 10^{-4}$ in the main text), and verified this power law over a wider range of α_L (Fig. S3).

Computing the steady state using variational matrix product states

The steady state of the Lindbladian system can be obtained by computing the eigenstate of the Lindblad operator \mathcal{L} corresponding to eigenvalue 0 (the system we studied has no degeneracy) [52, 53]. By rewriting the density operator ρ into a long vector, ρ could be written as a matrix product state, similar to a state vector of a unitary system. We use the variational matrix product states algorithm proposed in [52], where the iterative procedure to search for the steady state is done in the same way as the unitary case, except that one keeps the eigenstate corresponding to the eigenvalue with smallest magnitude

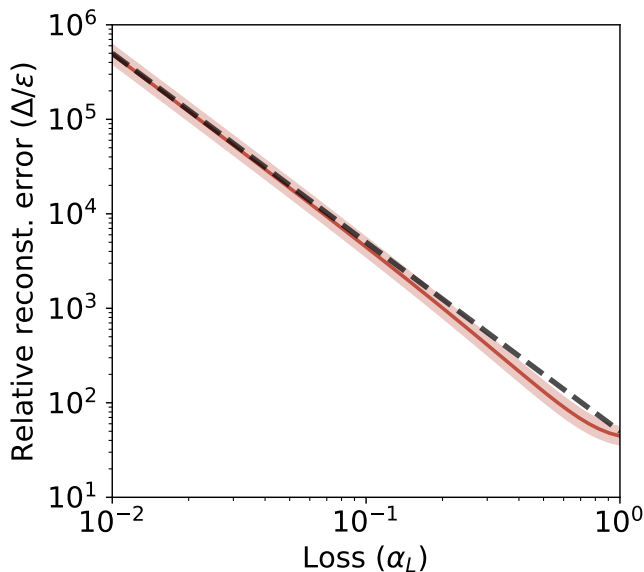


FIG. S3. Reconstruction error as a function of loss-to-dephasing ratio α_L . We repeated the simulations of Fig. 1c with lower measurement noise $\epsilon = 10^{-8}$ over a wider range of α_L . The dashed line follows the equation $y = 50x^{-2}$, confirming the theoretical expectation for the scaling of the reconstruction error with α_D .

instead of smallest algebraic value. For a system with 100 spins, we have used $D = 100$ number of states (bond dimension) for our simulations. We obtained a steady state with eigenvalue of the order 10^{-8} , and residual $\|\mathcal{L}\rho\| \approx 10^{-5}$. To check the convergence against different D s, we have done another simulation with $D = 150$, and compared the local observables $\langle \sigma_j^z \rangle$, obtaining a mean error $\sum_{j=1}^{\Lambda} |\langle \sigma_j^z \rangle_{D=100} - \langle \sigma_j^z \rangle_{D=150}| / \Lambda \approx 10^{-9}$. We also compared the distances between the reduced density matrices with a patching size 6, and a patching spacing 4, and obtained a mean error of the order of 10^{-8} .

Stitching up recovered patches

Recall that the Lindbladian on each patch is only recovered up to a multiplicative scalar. Suppose we recover the Lindbladian of two overlapping patches and wish to “stitch” them together into one Lindbladian acting on the joint patch. In the absence of noise, the recovered Lindbladians of the first two patches would be given by

$$\begin{cases} \vec{c}_l \cdot \mathcal{L}_l + \vec{c}_m \cdot \mathcal{L}_m \\ \vec{c}'_m \cdot \mathcal{L}_m + \vec{c}_r \cdot \mathcal{L}_r, \end{cases} \quad (\text{S8})$$

where \mathcal{L}_m is the vector of terms $[h_j]$ and pairs (l_r, l_s) acting on the overlapping region of the two patches; for the analysis below, we assume that each individual recovered Lindbladian is normalized: $\|\vec{c}_l\|^2 + \|\vec{c}_m\|^2 =$

$\|\vec{c}'_m\|^2 + \|\vec{c}_r\|^2 = 1$. The coefficients c_m, \vec{c}'_m of the overlapping region will generically differ since the Lindbladian on each patch is only recovered up to a multiplicative scalar. We therefore use these overlapping coefficients to determine the relative scale of the two patches, by multiplying the Lindbladian of the second patch by a factor of $\frac{\|\vec{c}_m\|}{\|\vec{c}'_m\|}$:

$$\mathcal{L}_{stitched} = \vec{c}_l \cdot \mathcal{L}_l + \vec{c}_m \cdot \mathcal{L}_m + \frac{\|\vec{c}_m\|}{\|\vec{c}'_m\|} \vec{c}_r \cdot \mathcal{L}_r. \quad (\text{S9})$$

In fact, we also need to fix the relative signs of the two patches using a similar factor of $\frac{\text{sign}(\vec{c}_m)}{\text{sign}(\vec{c}'_m)}$, where the sign can be determined e.g. according to the coefficient of a fixed shared term. While this last detail is crucial for the stitching process, it does not contribute to the recovery error due to noise, as long as the error in each patch is small relative to its size, so that no coefficient flips its sign.

To recover the Lindbladian of a sequence of patches $1, \dots, n$, we repeat this procedure iteratively and obtain

$$\mathcal{L}_{stitched}^{(n)} = \sum_{j=1}^n \mathcal{L}_{patch}^{(n)}, \quad (\text{S10})$$

where

$$\mathcal{L}_{patch}^{(1)} = \vec{c}_1 \cdot \mathcal{L}_1 + \vec{c}_{1,2} \cdot \mathcal{L}_{1,2}, \quad (\text{S11})$$

with $\mathcal{L}_{1,2}$ denoting the terms acting on the overlapping region of the first two patches. For any $j > 1$,

$$\mathcal{L}_{patch}^{(j)} = \left(\prod_{i=1}^{j-1} \frac{\|\vec{c}_{i,i+1}\|}{\|\vec{c}'_{i,i+1}\|} \right) (\vec{c}_j \cdot \mathcal{L}_j + \vec{c}_{j,j+1} \cdot \mathcal{L}_{j,j+1}). \quad (\text{S12})$$

If each individual patch is recovered perfectly up to a corresponding multiplicative scalar, this procedure yields the full system Lindbladian up to a single overall multiplicative scalar. However, noise introduces error in the recovered Lindbladian of each individual patch: $\vec{c}_j \mapsto \vec{c}_j + \vec{\delta}_j$.

Error in each individual patch affects the overall stitched Lindbladian in two ways. One effect is a rotation of each \mathcal{L}_{patch} with respect to its true value, the \mathcal{L}_j component pointing to $\vec{c}_j + \vec{\delta}_j$ rather than \vec{c}_j . Since this error is additive, it is absorbed in the normalization of $\mathcal{L}_{stitched}$; assuming that the error is approximately uniform across patches, $\|\vec{\delta}_j\| \approx \delta$, it leads to an overall error of order δ in the total $\mathcal{L}_{stitched}$, which is independent of the number of patches.

A second effect caused by the errors in the recovery of individual patches is a stretch of each \mathcal{L}_{patch} . This effect is induced through the errors' effect on the relative scale factor $\prod_{i=1}^{j-1} \frac{\|\vec{c}_{i,i+1}\|}{\|\vec{c}'_{i,i+1}\|}$. Assuming that the errors of the different patches $\vec{\delta}_j$ are independent, this scale factor

performs a multiplicative random walk, fluctuating from its true value by a deviation of order $\sqrt{j}\delta$. This is most easily seen by taking a log:

$$\log \left(\prod_{i=1}^{j-1} \frac{\|\vec{c}_{i,i+1} + \vec{\delta}_{i,i+1}\|}{\|\vec{c}'_{i,i+1} + \vec{\delta}'_{i,i+1}\|} \right) - \log \left(\prod_{i=1}^{j-1} \frac{\|\vec{c}_{i,i+1}\|}{\|\vec{c}'_{i,i+1}\|} \right) \quad (\text{S13})$$

$$= \sum_{i=1}^{j-1} \left(\log \frac{\|\vec{c}_{i,i+1} + \vec{\delta}_{i,i+1}\|}{\|\vec{c}_{i,i+1}\|} - \log \frac{\|\vec{c}'_{i,i+1} + \vec{\delta}'_{i,i+1}\|}{\|\vec{c}'_{i,i+1}\|} \right). \quad (\text{S14})$$

To first order in δ , each of these is an independent random variable with zero mean and standard deviation of order δ :

$$\begin{aligned} \log \frac{\|\vec{c}_{i,i+1} + \vec{\delta}_{i,i+1}\|}{\|\vec{c}_{i,i+1}\|} &= \\ &= \log \left(1 + \hat{c}_{i,i+1} \cdot \vec{\delta}_{i,i+1} + O(\delta^2) \right) \approx \hat{c}_{i,i+1} \cdot \vec{\delta}_{i,i+1} \end{aligned}$$

where $\hat{c}_{i,i+1} = \vec{c}_{i,i+1}/\|\vec{c}_{i,i+1}\|$. Therefore, the ratio between the true scale factor and its noisy version is given by $e^{\tilde{\delta}}$, where $\tilde{\delta}$ is the random variable given by Eq. (S14). Its standard deviation scales as $\sqrt{j}\delta \leq \sqrt{n}\delta$, where n is the total number of patches. While the order δ^2 correction is always positive, resulting in a drift, it sums up across the patches to $O(n\delta^2)$, and is therefore higher order in $\sqrt{n}\delta$. Thus, as long as $\sqrt{n}\delta \ll 1$, the Lindbladian on each patch is stretched by a factor of at most $\approx 1 \pm \sqrt{n}\delta$, leading to a total recovery error of order $\sqrt{n}\delta$. This explains the square root scaling of the error with system size seen in Fig. 3.